



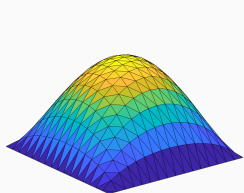
Fast and Robust Overlapping Schwarz (FROSch) Domain Decomposition Preconditioners

Alexander Heinlein¹

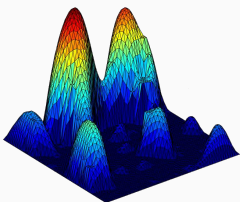
High Performance Computing in Science and Engineering 2024 conference (HPCSE 2024), Beskydy,
Czech Republic, May 20 - 23, 2024

¹Delft University of Technology

Solving A Model Problem



$$\alpha(x) = 1$$



$$\text{heterogeneous } \alpha(x)$$

Consider a **diffusion model problem**:

$$\begin{aligned} -\nabla \cdot (\alpha(x) \nabla u(x)) &= f \quad \text{in } \Omega = [0, 1]^2, \\ u &= 0 \quad \text{on } \partial\Omega. \end{aligned}$$

Discretization using finite elements yields a **sparse** linear system of equations

$$\mathbf{K}\mathbf{u} = \mathbf{f}.$$

⇒ We introduce a preconditioner $\mathbf{M}^{-1} \approx \mathbf{A}^{-1}$ to improve the condition number:

$$\mathbf{M}^{-1} \mathbf{A} \mathbf{u} = \mathbf{M}^{-1} \mathbf{f}$$

Direct solvers

For fine meshes, solving the system using a direct solver is not feasible due to **superlinear complexity and memory cost**.

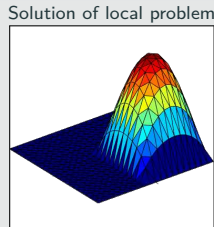
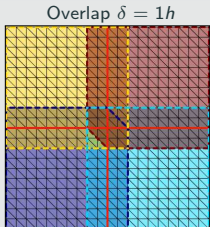
Iterative solvers

Iterative solvers are efficient for solving sparse linear systems of equations, however, the **convergence rate generally depends on the condition number $\kappa(\mathbf{A})$** . It deteriorates, e.g., for

- fine meshes, that is, small element sizes h
- large contrasts $\frac{\max_x \alpha(x)}{\min_x \alpha(x)}$

Two-Level Schwarz Preconditioners

One-level Schwarz preconditioner



Based on an **overlapping domain decomposition**, we define a **one-level Schwarz operator**

$$M_{OS-1}^{-1} K = \sum_{i=1}^N R_i^\top K_i^{-1} R_i K,$$

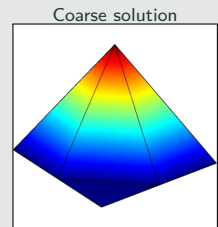
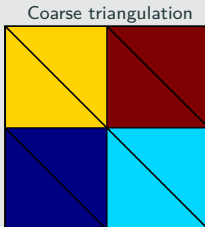
where R_i and R_i^\top are restriction and prolongation operators corresponding to Ω'_i , and $K_i := R_i K R_i^\top$.

Condition number estimate:

$$\kappa(M_{OS-1}^{-1} K) \leq C \left(1 + \frac{1}{H\delta} \right)$$

with subdomain size H and overlap width δ .

Lagrangian coarse space



The **two-level overlapping Schwarz operator** reads

$$M_{OS-2}^{-1} K = \underbrace{\Phi K_0^{-1} \Phi^\top K}_{\text{coarse level - global}} + \underbrace{\sum_{i=1}^N R_i^\top K_i^{-1} R_i K}_{\text{first level - local}},$$

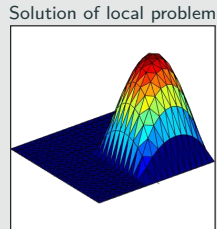
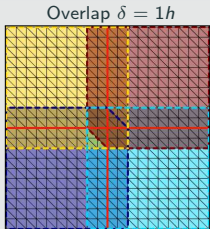
where Φ contains the coarse basis functions and $K_0 := \Phi^\top K \Phi$; cf., e.g., [Toselli, Widlund \(2005\)](#).
The construction of a Lagrangian coarse basis requires a coarse triangulation.

Condition number estimate:

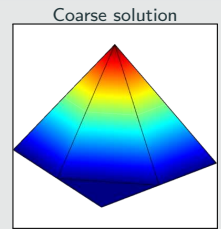
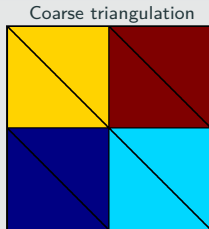
$$\kappa(M_{OS-2}^{-1} K) \leq C \left(1 + \frac{H}{\delta} \right)$$

Two-Level Schwarz Preconditioners

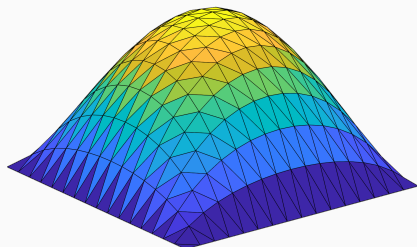
One-level Schwarz preconditioner



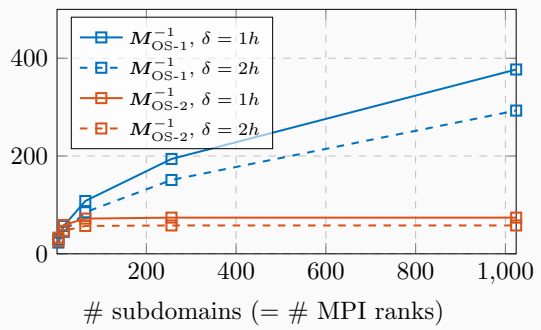
Lagrangian coarse space



Diffusion model problem in two dimensions,
 $H/h = 100$



iterations



FROSCh (Fast and Robust Overlapping Schwarz) Framework in Trilinos



Software

- Object-oriented C++ domain decomposition solver framework with MPI-based distributed memory parallelization
- Part of TRILINOS with support for both parallel linear algebra packages EPETRA and TPETRA
- Node-level parallelization and performance portability on CPU and GPU architectures through KOKKOS and KOKKOSKERNELS
- Accessible through unified TRILINOS solver interface STRATIMIKOS

Methodology

- Parallel scalable multi-level Schwarz domain decomposition preconditioners
- Algebraic construction based on the parallel distributed system matrix
- Extension-based coarse spaces

Team (active)

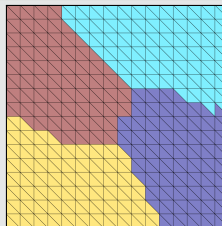
- | | |
|---------------------------------|---------------------------------|
| ▪ Filipe Cumaru (TU Delft) | ▪ Alexander Heinlein (TU Delft) |
| ▪ Kyrill Ho (UCologne) | ▪ Axel Klawonn (UCologne) |
| ▪ Jascha Knepper (UCologne) | ▪ Siva Rajamanickam (SNL) |
| ▪ Friederike Röver (TUBAF) | ▪ Oliver Rheinbach (TUBAF) |
| ▪ Lea Saßmannshausen (UCologne) | ▪ Ichitaro Yamazaki (SNL) |

Algorithmic Framework for FROSch Preconditioners

Overlapping domain decomposition

Adjacency can be determined algebraically from the sparsity pattern of the system matrix \mathbf{A} (nonzero off-diagonal entries).

Nonoverlapping DD

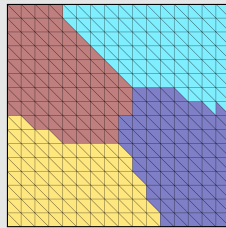


Algorithmic Framework for FROSch Preconditioners

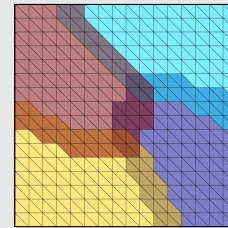
Overlapping domain decomposition

Adjacency can be determined algebraically from the sparsity pattern of the system matrix \mathbf{A} (nonzero off-diagonal entries).

Nonoverlapping DD



Overlap $\delta = 1h$

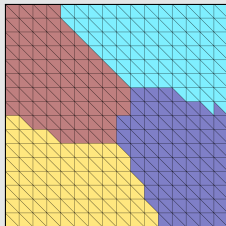


Algorithmic Framework for FROSch Preconditioners

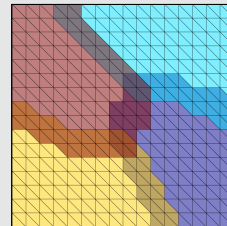
Overlapping domain decomposition

Adjacency can be determined algebraically from the sparsity pattern of the system matrix \mathbf{A} (nonzero off-diagonal entries).

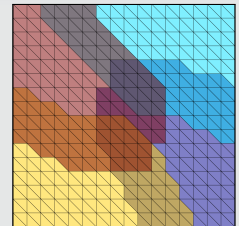
Nonoverlapping DD



Overlap $\delta = 1h$



Overlap $\delta = 2h$

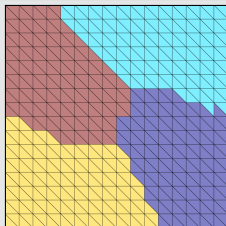


Algorithmic Framework for FROSch Preconditioners

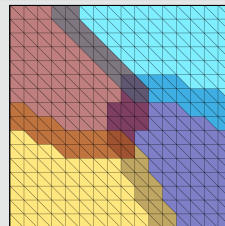
Overlapping domain decomposition

Adjacency can be determined algebraically from the sparsity pattern of the system matrix \mathbf{A} (nonzero off-diagonal entries).

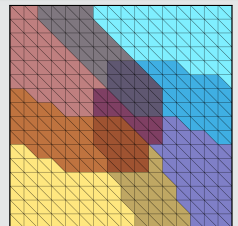
Nonoverlapping DD



Overlap $\delta = 1h$

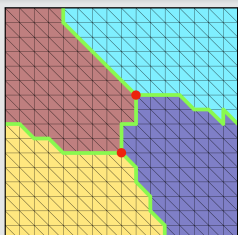


Overlap $\delta = 2h$

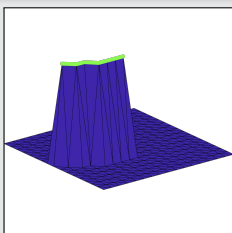


Coarse space

1. Interface components

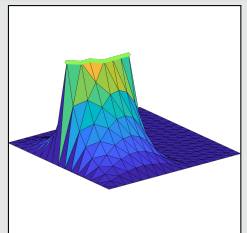


2. Interface basis (partition of unity \times null space)



For scalar elliptic problems, the null space consists only of constant functions.

3. Extension

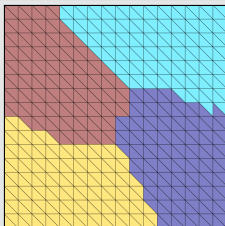


Algorithmic Framework for FROSch Preconditioners

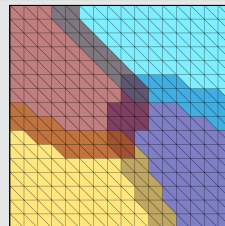
Overlapping domain decomposition

Adjacency can be determined algebraically from the sparsity pattern of the system matrix \mathbf{A} (nonzero off-diagonal entries).

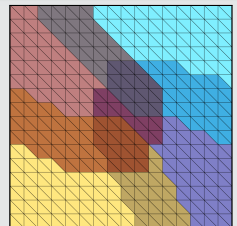
Nonoverlapping DD



Overlap $\delta = 1h$

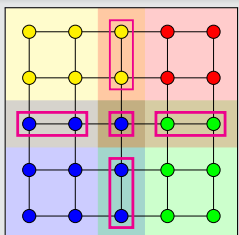


Overlap $\delta = 2h$

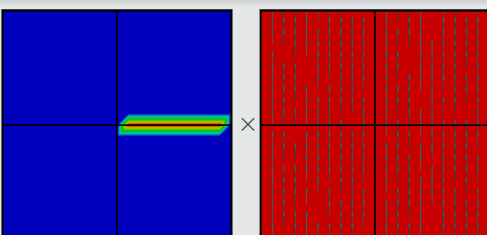


Coarse space

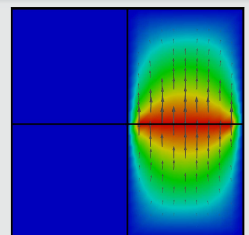
1. Interface components



2. Interface basis (partition of unity \times null space)

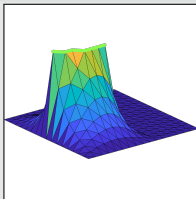
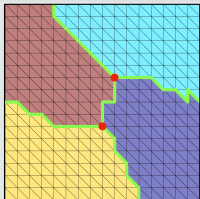


3. Extension



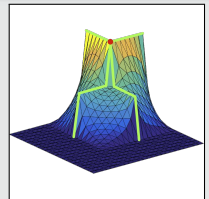
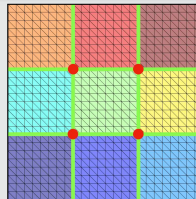
Examples of FROSch Coarse Spaces

GDSW (Generalized Dryja–Smith–Widlund)



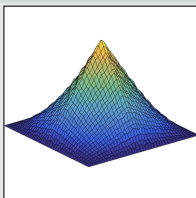
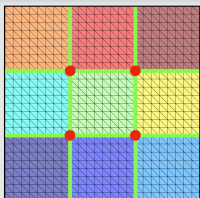
- Dohrmann, Klawonn, Widlund (2008)
- Dohrmann, Widlund (2009, 2010, 2012)

RGDSW (Reduced dimension GDSW)



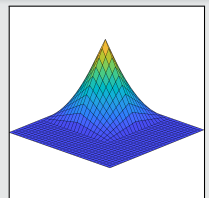
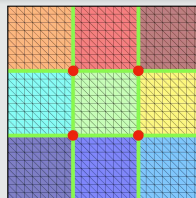
- Dohrmann, Widlund (2017)
- H., Klawonn, Knepper, Rheinbach, Widlund (2022)

MsFEM (Multiscale Finite Element Method)



- Hou (1997), Efendiev and Hou (2009)
- Buck, Iliev, and Andrä (2013)
- H., Klawonn, Knepper, Rheinbach (2018)

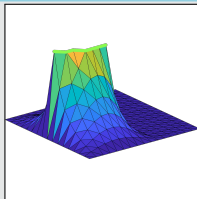
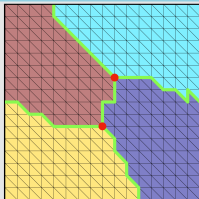
Q1 Lagrangian / piecewise bilinear



Piecewise linear interface partition of unity functions and a structured domain decomposition.

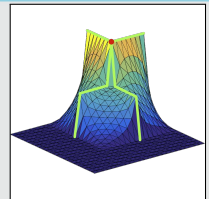
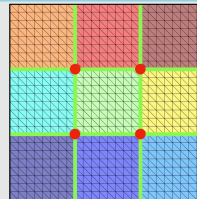
Examples of FROSch Coarse Spaces

GDSW (Generalized Dryja–Smith–Widlund)



- Dohrmann, Klawonn, Widlund (2008)
- Dohrmann, Widlund (2009, 2010, 2012)

RGDSW (Reduced dimension GDSW)



- Dohrmann, Widlund (2017)
- H., Klawonn, Knepper, Rheinbach, Widlund (2022)

For elliptic model problems, the **condition number** of the (R)GDSW two-level Schwarz operator is bounded by

$$\kappa \left(\mathbf{M}_{(\text{R})\text{GDSW}}^{-1} \mathbf{K} \right) \leq C \left(1 + \frac{H}{\delta} \right) \left(1 + \log \left(\frac{H}{h} \right) \right)^\alpha,$$

where

C constant (does not depend on h , H , or δ),

H subdomain diameter,

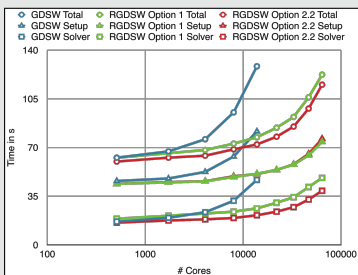
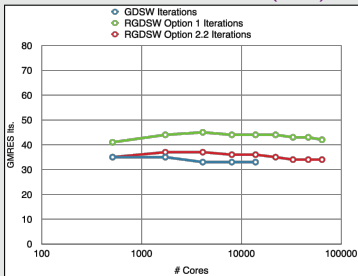
h element size,

δ width of the overlap,

$\alpha \in \{0, 1, 2\}$ power (depends on problem dimension, regularity of the subdomains, and variant of the algorithm).

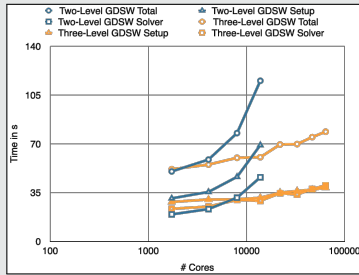
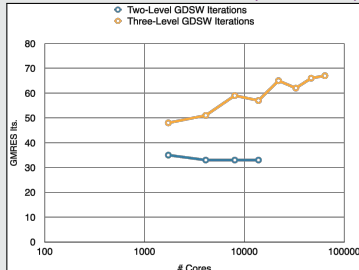
GDSW vs RGDSW (reduced dimension)

Heinlein, Klawonn, Rheinbach, Widlund (2019).



Two-level vs three-level GDSW

Heinlein, Klawonn, Rheinbach, Röver (2019, 2020).



Monolithic and Adaptive Extension-Based Coarse Spaces

Monolithic (R)GDSW Preconditioners for CFD Simulations

Consider the discrete saddle point problem

$$\mathcal{A}x = \begin{bmatrix} K & B^\top \\ B & 0 \end{bmatrix} \begin{bmatrix} u \\ p \end{bmatrix} = \begin{bmatrix} f \\ 0 \end{bmatrix} = b.$$

Monolithic GDSW preconditioner

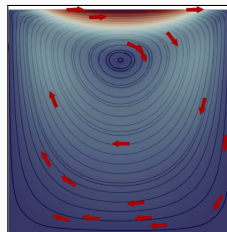
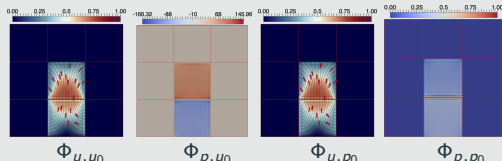
We construct a **monolithic GDSW preconditioner**

$$m_{\text{GDSW}}^{-1} = \phi \mathcal{A}_0^{-1} \phi^\top + \sum_{i=1}^N \mathcal{R}_i^\top \mathcal{A}_i^{-1} \mathcal{R}_i,$$

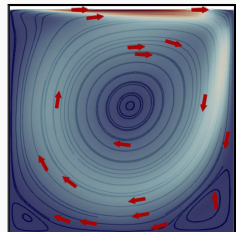
with block matrices $\mathcal{A}_0 = \phi^\top \mathcal{A} \phi$, $\mathcal{A}_i = \mathcal{R}_i \mathcal{A} \mathcal{R}_i^\top$, and

$$\mathcal{R}_i = \begin{bmatrix} \mathcal{R}_{u,i} & \mathbf{0} \\ \mathbf{0} & \mathcal{R}_{p,i} \end{bmatrix} \quad \text{and} \quad \phi = \begin{bmatrix} \Phi_{u,u_0} & \Phi_{u,p_0} \\ \Phi_{p,u_0} & \Phi_{p,p_0} \end{bmatrix}.$$

Using \mathcal{A} to compute extensions: $\phi_I = -\mathcal{A}_{II}^{-1} \mathcal{A}_{I\Gamma} \phi_\Gamma$; cf. [Heinlein, Hochmuth, Klawonn \(2019, 2020\)](#).



Stokes flow



Navier–Stokes flow

Related work:

- Original work on monolithic Schwarz preconditioners: [Klawonn and Pavarino \(1998, 2000\)](#)
- Other publications on monolithic Schwarz preconditioners: e.g., [Hwang and Cai \(2006\)](#), [Barker and Cai \(2010\)](#), [Wu and Cai \(2014\)](#), and the presentation [Dohrmann \(2010\)](#) at the *Workshop on Adaptive Finite Elements and Domain Decomposition Methods* in Milan.

Monolithic (R)GDSW Preconditioners for CFD Simulations

Consider the discrete saddle point problem

$$\mathcal{A}x = \begin{bmatrix} K & B^\top \\ B & 0 \end{bmatrix} \begin{bmatrix} u \\ p \end{bmatrix} = \begin{bmatrix} f \\ 0 \end{bmatrix} = b.$$

Monolithic GDSW preconditioner

We construct a **monolithic GDSW preconditioner**

$$m_{\text{GDSW}}^{-1} = \phi \mathcal{A}_0^{-1} \phi^\top + \sum_{i=1}^N \mathcal{R}_i^\top \mathcal{A}_i^{-1} \mathcal{R}_i,$$

with block matrices $\mathcal{A}_0 = \phi^\top \mathcal{A} \phi$, $\mathcal{A}_i = \mathcal{R}_i \mathcal{A} \mathcal{R}_i^\top$.

SIMPLE block preconditioner

We employ the **SIMPLE (Semi-Implicit Method for Pressure Linked Equations)** block preconditioner

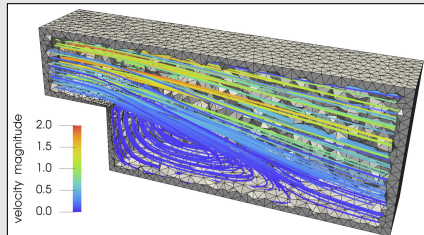
$$m_{\text{SIMPLE}}^{-1} = \begin{bmatrix} I & -D^{-1}B \\ 0 & \alpha I \end{bmatrix} \begin{bmatrix} K^{-1} & 0 \\ -\hat{S}^{-1}BK^{-1} & \hat{S}^{-1} \end{bmatrix};$$

see **Patankar and Spalding (1972)**. Here,

- $\hat{S} = -BD^{-1}B^\top$, with $D = \text{diag } K$
- α is an under-relaxation parameter

We **approximate the inverses** using (R)GDSW preconditioners.

Monolithic vs. SIMPLE preconditioner

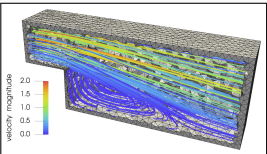
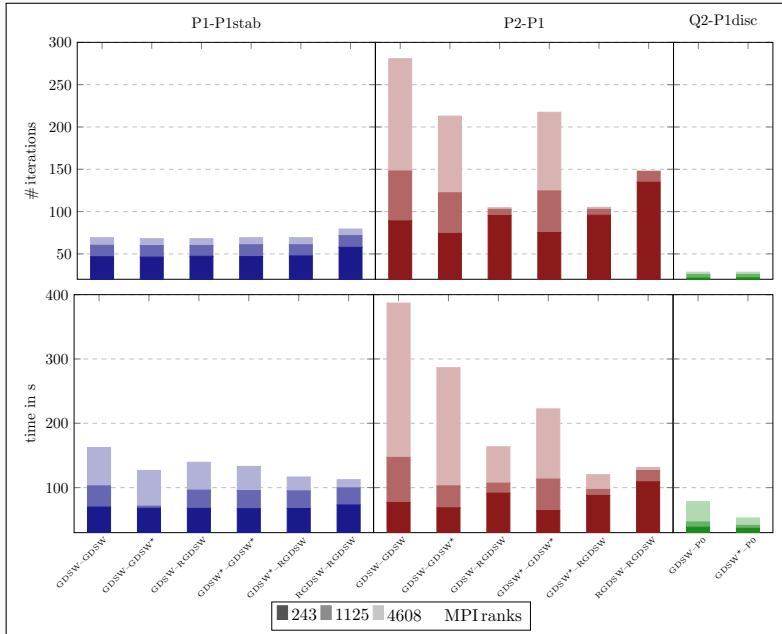


Steady-state Navier–Stokes equations

prec.	# MPI ranks	243	1 125	15 562
Monolithic	setup	39.6 s	57.9 s	95.5 s
	solve	57.6 s	69.2 s	74.9 s
	total	97.2 s	127.7 s	170.4 s
SIMPLE	setup	39.2 s	38.2 s	68.6 s
	solve	86.2 s	106.6 s	127.4 s
	total	125.4 s	144.8 s	196.0 s

Computations on Piz Daint (CSCS). Implementation in the finite element software FEDDLib.

Balancing the Velocity and Pressure Coarse Spaces



Varying the POU



Local Pressure Projections

We slightly modify the monolithic two-level overlapping Schwarz preconditioner

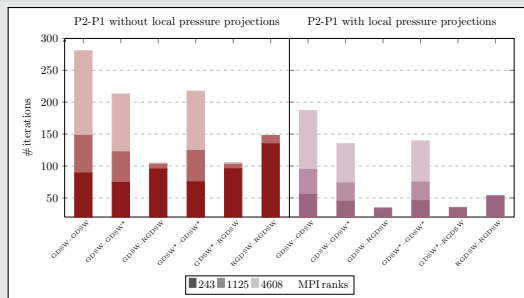
$$m_{\text{OS-2}}^{-1} = \phi \mathcal{A}_0^{-1} \phi^\top + \sum_{i=1}^N \mathcal{R}_i^\top \bar{\mathcal{P}}_i \mathcal{A}_i^{-1} \mathcal{R}_i,$$

with local projection operators $\bar{\mathcal{P}}_i$ of the form

$$\bar{\mathcal{P}}_i = \begin{bmatrix} I_{u,i} & 0 \\ 0 & \bar{P}_{p,i} \end{bmatrix}, \text{ with } \bar{P}_{p,i} = I_{p,i} - \frac{a_i a_i^T}{a_i^T a_i},$$

where a_i is the discretization of the integral $\int_{\Omega_i} u \, dx$.

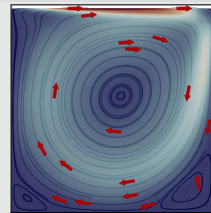
Backward-facing step (Re = 200)



Computations on Fritz (FAU).

Alexander Heinlein (Delft University of Technology)

Lid-driven cavity Stokes



Navier–Stokes flow with kinematic viscosity $\nu = 1e^{-3}$

# MPI ranks	196	1 089	4 356	
P2-P1, H/h = 50	Local projections —	33 118	36 172	35 237
P1-P1stab H/h = 80	Pressure stab.	38	36	36

RGDSW–RGDSW coarse spaces

→ Local pressure corrections significantly improve the convergence. We obtain very fast convergence using a good combination of coarse spaces.

Heinlein, Klawonn, Saßmannshausen (in prep.)

HPCSE 2024

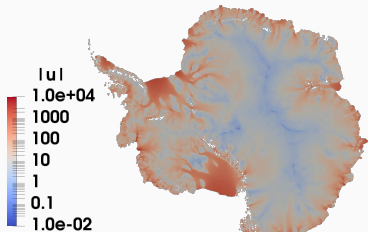
FROSch Preconditioners for Land Ice Simulations



<https://github.com/SNLComputation/Albany>

The velocity of the ice sheet in Antarctica and Greenland is modeled by a **first-order-accurate Stokes approximation model**,

$$-\nabla \cdot (2\mu \dot{\epsilon}_1) + \rho g \frac{\partial s}{\partial x} = 0, \quad -\nabla \cdot (2\mu \dot{\epsilon}_2) + \rho g \frac{\partial s}{\partial y} = 0,$$



with a **nonlinear viscosity model** (Glen's law); cf., e.g., **Blatter (1995)** and **Pattyn (2003)**.

MPI ranks	Antarctica (velocity)			Greenland (multiphysics vel. & temperature)				
	4 km resolution, 20 layers, 35 m dofs	avg. its	avg. setup	avg. solve	1-10 km resolution, 20 layers, 69 m dofs	avg. its	avg. setup	avg. solve
512	41.9 (11)	25.10 s	12.29 s	12.29 s	41.3 (36)	18.78 s	4.99 s	4.99 s
1 024	43.3 (11)	9.18 s	5.85 s	5.85 s	53.0 (29)	8.68 s	4.22 s	4.22 s
2 048	41.4 (11)	4.15 s	2.63 s	2.63 s	62.2 (86)	4.47 s	4.23 s	4.23 s
4 096	41.2 (11)	1.66 s	1.49 s	1.49 s	68.9 (40)	2.52 s	2.86 s	2.86 s
8 192	40.2 (11)	1.26 s	1.06 s	1.06 s	-	-	-	-

Computations performed on Cori (NERSC).

Heinlein, Perego, Rajamanickam (2022)

Adaptive Extension-Based Coarse Spaces for Schwarz Preconditioners

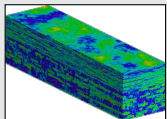
Highly heterogeneous problems . . .

. . . appear in most areas of modern science and engineering:

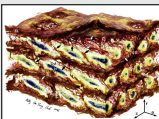


Micro section of a dual-phase steel.

Courtesy of J. Schröder.



Groundwater flow (SPE10);
cf. Christie and Blunt (2001).



Composition of arterial walls; taken from O'Connell et al. (2008).

Adaptive coarse spaces

The coarse space is enhanced by eigenfunctions of **local edge and face eigenvalue problems** with eigenvalues below tolerances $tol_{\mathcal{E}}$ and $tol_{\mathcal{F}}$:

$$\kappa(M_*^{-1}K) \leq C \left(1 + \frac{1}{tol_{\mathcal{E}}} + \frac{1}{tol_{\mathcal{F}}} + \frac{1}{tol_{\mathcal{E}} \cdot tol_{\mathcal{F}}} \right);$$

C does not depend on h , H , or the coefficients.

OS-ACMS & adaptive GDSW (AGDSW) (Heinlein, Klawonn, Knepper, Rheinbach (2018, 2018, 2019)).

Local eigenvalue problems

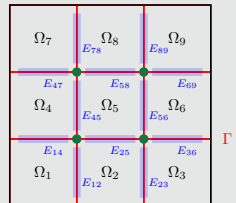
Local generalized eigenvalue problems corresponding to the edges \mathcal{E} and faces \mathcal{F} of the domain decomposition:

$$\forall E \in \mathcal{E}: \quad S_{EE}\tau_{*,E} = \lambda_{*,E} K_{EE}\tau_{*,E}, \quad \forall \tau_{*,E} \in V_E,$$

$$\forall F \in \mathcal{F}: \quad S_{FF}\tau_{*,F} = \lambda_{*,F} K_{FF}\tau_{*,F}, \quad \forall \tau_{*,F} \in V_F,$$

with **Schur complements** S_{EE} , S_{FF} with **Neumann boundary conditions** and submatrices K_{EE} , K_{FF} of K . We select eigenfunctions corresponding to **eigenvalues below tolerances** $tol_{\mathcal{E}}$ and $tol_{\mathcal{F}}$.

→ The corresponding coarse basis functions are **energy-minimizing extensions** into the interior of the subdomains.



Adaptive Extension-Based Coarse Spaces for Schwarz Preconditioners

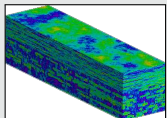
Highly heterogeneous problems . . .

. . . appear in most areas of modern science and engineering:

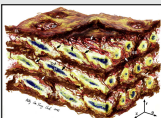


Micro section of a dual-phase steel.

Courtesy of J. Schröder.



Groundwater flow (SPE10);
cf. Christie and Blunt (2001).



Composition of arterial walls; taken from O'Connell et al. (2008).

Adaptive coarse spaces

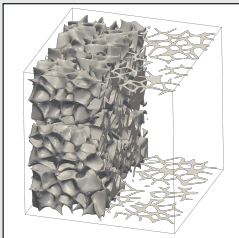
The coarse space is enhanced by eigenfunctions of **local edge and face eigenvalue problems** with eigenvalues below tolerances $tol_{\mathcal{E}}$ and $tol_{\mathcal{F}}$:

$$\kappa(M_*^{-1}K) \leq C \left(1 + \frac{1}{tol_{\mathcal{E}}} + \frac{1}{tol_{\mathcal{F}}} + \frac{1}{tol_{\mathcal{E}} \cdot tol_{\mathcal{F}}} \right);$$

C does not depend on h , H , or the coefficients.

OS-ACMS & adaptive GDSW (AGDSW) (Heinlein, Klawonn, Knepper, Rheinbach (2018, 2018, 2019)).

Foam coefficient function example



Solid phase: $A = 10^6$; transparent phase: $A = 1$; 100 subdomains

V_0	$tol_{\mathcal{E}}$	$tol_{\mathcal{F}}$	it.	κ	$\dim V_0$	$\dim V_0 / \text{dof}$
V_{GDSW}	—	—	565	$1.3 \cdot 10^6$	1601	0.27 %
V_{AGDSW}	0.05	0.05	60	30.2	1968	0.33 %
$V_{\text{OS-ACMS}}$	0.001	0.001	57	30.3	690	0.12 %

Cf. Heinlein, Klawonn, Knepper, Rheinbach (2018, 2019).

Algebraic Adaptive Extension-Based Coarse Spaces

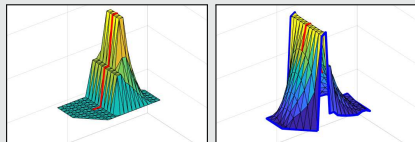
Two algebraic eigenvalue problems

Use the a -orthogonal decomposition

$$V_{\Omega_e} = V_{\Omega_e}^0 \oplus \{E_{\partial\Omega_e \rightarrow \Omega_e}(v) : v \in V_{\partial\Omega_e}\}$$

to “**split the AGDSW (Neumann) eigenvalue problem**” into two:

- Dirichlet eigenvalue problem on $V_{\Omega_e}^0$
- Transfer eigenvalue problem on $V_{\Omega_e, \text{harm}}$; cf. [Smetana, Patera \(2016\)](#)



Condition number estimate

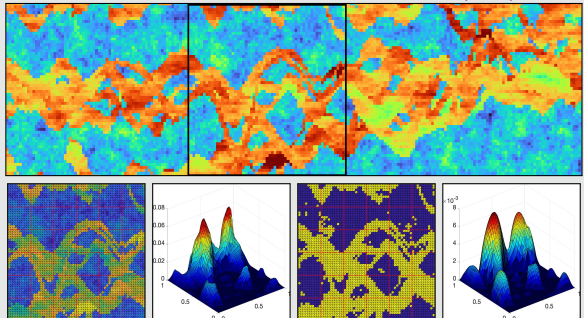
$$\kappa(M_{\text{DIR\&TR}}^{-1} K) \leq C \max \{1/TOL_{\text{DIR}}, TOL_{\text{TR}}/\alpha_{\min}\},$$

where C is independent of H , h , and the contrast of the coefficient function α .

[Heinlein & Smetana \(subm. 2023; preprint arXiv\)](#).

Numerical results – SPE10 benchmark

Layer 70 from model 2; cf. [Christie and Blunt \(2001\)](#)



V_0	TOL_{DIR}	TOL_{TR}	$\dim V_0$	κ	its.
V_{GDSW}	-	-	85	$2.0 \cdot 10^5$	57
V_{AGDSW}	$1.0 \cdot 10^{-2}$		93	19.3	38
$V_{\text{DIR\&TR-}a}$	$1.0 \cdot 10^{-3}$	$1.0 \cdot 10^5$	90	19.4	39
$V_{\text{DIR\&TR-}l^2}$	$1.0 \cdot 10^{-3}$	$1.0 \cdot 10^5$	147	9.6	31

Original coefficient (without thresholding)					
V_{GDSW}	-	-	85	20.6	42

Accelerating Time-to-Solution

Inexact Subdomain Solvers in FROSch

$$\mathbf{M}_{\text{OS-2}}^{-1} \mathbf{K} = \Phi \mathbf{K}_0^{-1} \Phi^T \mathbf{K} + \sum_{i=1}^N \mathbf{R}_i^T \mathbf{K}_i^{-1} \mathbf{R}_i \mathbf{K}$$

3D Laplacian; 512 MPI ranks = 512 ($= 8 \times 8 \times 8$) subdomains; $H/\delta = 10$; RGDSW coarse space.

		subdomain solver						
		direct solver	ILU(k)		symm. Gauß–Seidel		Chebyshev polyn.	
			k = 2	k = 3	5 sweeps	10 sweeps	p = 6	p = 8
$H/h = 20$, $\approx 14 k$ dofs per rank	iter	26	33	30	31	28	34	31
	setup time	1.89 s	0.97 s	1.01 s	0.89 s	0.91 s	0.73 s	0.71 s
	apply time	0.39 s	0.27 s	0.31 s	0.31 s	0.35 s	0.30 s	0.30 s
	prec. time	2.28 s	1.24 s	1.32 s	1.20 s	1.26 s	1.03 s	1.01 s
$H/h = 40$, $\approx 105 k$ dofs per rank	iter	30	55	46	52	41	59	51
	setup time	12.09 s	6.14 s	6.26 s	5.74 s	5.89 s	5.55 s	5.64 s
	apply time	4.21 s	1.84 s	1.96 s	2.66 s	3.28 s	2.52 s	2.47 s
	prec. time	16.30 s	7.98 s	8.22 s	8.40 s	9.18 s	8.16 s	8.11 s
$H/h = 60$, $\approx 350 k$ dofs per rank	iter		81	64	76	56	88	74
	setup time	OOM	47.29 s	47.87 s	45.14 s	45.08 s	45.44 s	45.49 s
	apply time		10.79 s	9.98 s	13.00 s	16.16 s	11.95 s	12.09 s
	prec. time		58.08 s	57.85 s	58.15 s	61.25 s	57.39 s	57.59 s

INTEL MKL PARDISO; ILU / symmetric Gauß–Seidel / Chebyshev polynomials from IFPACK2.

Parallel computations on dual-socket Intel Xeon Platinum machine at Sandia National Laboratories (Blake).

Inexact Subdomain Solvers in FROSch

$$\mathbf{M}_{\text{OS-2}}^{-1} \mathbf{K} = \Phi \mathbf{K}_0^{-1} \Phi^T \mathbf{K} + \sum_{i=1}^N \mathbf{R}_i^T \mathbf{K}_i^{-1} \mathbf{R}_i \mathbf{K}$$

3D Laplacian; 512 MPI ranks = 512 ($= 8 \times 8 \times 8$) subdomains; $H/\delta = 10$; RGDSW coarse space.

		subdomain solver							
		direct solver	ILU(k)		symm. Gauß–Seidel		Chebyshev polyn.		
			k = 2	k = 3	5 sweeps	10 sweeps	p = 6	p = 8	
$H/h = 20,$ $\approx 14 k$ dofs per rank	iter	26	33	30	31	28	34	31	
	setup time	1.89 s	0.97 s	1.01 s	0.89 s	0.91 s	0.73 s	0.71 s	
	apply time	0.39 s	0.27 s	0.31 s	0.31 s	0.35 s	0.30 s	0.30 s	
	prec. time	2.28 s	1.24 s	1.32 s	1.20 s	1.26 s	1.03 s	1.01 s	
$H/h = 40,$ $\approx 105 k$ dofs per rank	iter	30	55	46	52	41	59	51	
	setup time	12.09 s	6.14 s	6.26 s	5.74 s	5.89 s	5.55 s	5.64 s	
	apply time	4.21 s	1.84 s	1.96 s	2.66 s	3.28 s	2.52 s	2.47 s	
	prec. time	16.30 s	7.98 s	8.22 s	8.40 s	9.18 s	8.16 s	8.11 s	
$H/h = 60,$ $\approx 350 k$ dofs per rank	iter		81	64	76	56	88	74	
	setup time	OOM	47.29 s	47.87 s	45.14 s	45.08 s	45.44 s	45.49 s	
	apply time		10.79 s	9.98 s	13.00 s	16.16 s	11.95 s	12.09 s	
	prec. time		58.08 s	57.85 s	58.15 s	61.25 s	57.39 s	57.59 s	

INTEL MKL PARDISO; ILU / symmetric Gauß–Seidel / Chebyshev polynomials from IFPACK2.

Parallel computations on dual-socket Intel Xeon Platinum machine at Sandia National Laboratories (Blake).

Inexact Extension Solvers in FROSch

$$\Phi = \begin{bmatrix} -\mathbf{K}_{\Pi\Pi}^{-1} \mathbf{K}_{\Gamma\Pi}^T \Phi_{\Gamma} \\ \Phi_{\Gamma} \end{bmatrix} = \begin{bmatrix} \Phi_I \\ \Phi_{\Gamma} \end{bmatrix}$$

3D Laplacian; 512 MPI ranks = 512 ($= 8 \times 8 \times 8$) subdomains; $H/\delta = 10$; RGDSW coarse space.

extension solver (10 Gauss-Seidel sweeps for the subdomain solver)	direct solver	preconditioned GMRES (rel. tol. = 10^{-4})					
		ILU(k)		symm. Gauß-Seidel		Chebyshev polyn.	
		k = 2	k = 3	5 sweeps	10 sweeps	p = 6	p = 8
$H/h = 20$, $\approx 14 k$ dofs per rank	iter	28	28	28	28	28	28
	setup time	0.89 s	0.93 s	0.89 s	0.78 s	0.83 s	0.79 s
	apply time	0.35 s	0.35 s	0.34 s	0.36 s	0.34 s	0.35 s
	prec. time	1.23 s	1.28 s	1.23 s	1.14 s	1.17 s	1.14 s
$H/h = 40$, $\approx 105 k$ dofs per rank	iter	41	41	41	41	41	41
	setup time	5.72 s	4.16 s	4.61 s	4.26 s	4.64 s	4.27 s
	apply time	3.33 s	3.33 s	3.30 s	3.33 s	3.30 s	3.28 s
	prec. time	9.04 s	7.49 s	7.92 s	7.59 s	7.95 s	7.55 s
$H/h = 60$, $\approx 350 k$ dofs per rank	iter	56	56	56	56	56	56
	setup time	45.16 s	17.75 s	18.16 s	17.98 s	19.34 s	17.93 s
	apply time	15.83 s	18.04 s	17.08 s	16.26 s	15.81 s	16.19 s
	prec. time	60.99 s	35.79 s	35.25 s	34.24 s	35.15 s	34.12 s

INTEL MKL PARDISO; ILU / symmetric Gauß-Seidel / Chebyshev polynomials from IFPACK2.

Parallel computations on dual-socket Intel Xeon Platinum machine at Sandia National Laboratories (Blake).

Inexact Extension Solvers in FROSch

$$\Phi = \begin{bmatrix} -\mathbf{K}_{II}^{-1} \mathbf{K}_{I\Gamma}^T \Phi_{\Gamma} \\ \Phi_{\Gamma} \end{bmatrix} = \begin{bmatrix} \Phi_I \\ \Phi_{\Gamma} \end{bmatrix}$$

3D Laplacian; 512 MPI ranks = 512 ($= 8 \times 8 \times 8$) subdomains; $H/\delta = 10$; RGDSW coarse space.

extension solver (10 Gauss-Seidel sweeps for the subdomain solver)	direct solver	preconditioned GMRES (rel. tol. = 10^{-4})					
		ILU(k)		symm. Gauß-Seidel		Chebyshev polyn.	
		k = 2	k = 3	5 sweeps	10 sweeps	p = 6	p = 8
$H/h = 20$, $\approx 14 k$ dofs per rank	iter	28	28	28	28	28	28
	setup time	0.89 s	0.93 s	0.89 s	0.78 s	0.83 s	0.79 s
	apply time	0.35 s	0.35 s	0.34 s	0.36 s	0.34 s	0.35 s
	prec. time	1.23 s	1.28 s	1.23 s	1.14 s	1.17 s	1.14 s
$H/h = 40$, $\approx 105 k$ dofs per rank	iter	41	41	41	41	41	41
	setup time	5.72 s	4.16 s	4.61 s	4.26 s	4.64 s	4.27 s
	apply time	3.33 s	3.33 s	3.30 s	3.33 s	3.30 s	3.28 s
	prec. time	9.04 s	7.49 s	7.92 s	7.59 s	7.95 s	7.55 s
$H/h = 60$, $\approx 350 k$ dofs per rank	iter	56	56	56	56	56	56
	setup time	45.16 s	17.75 s	18.16 s	17.98 s	19.34 s	17.93 s
	apply time	15.83 s	18.04 s	17.08 s	16.26 s	15.81 s	16.19 s
	prec. time	60.99 s	35.79 s	35.25 s	34.24 s	35.15 s	34.12 s

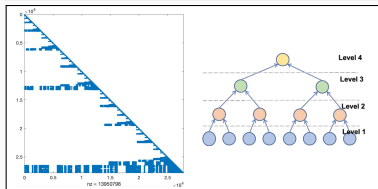
INTEL MKL PARDISO; ILU / symmetric Gauß-Seidel / Chebyshev polynomials from IFPACK2.

Parallel computations on dual-socket Intel Xeon Platinum machine at Sandia National Laboratories (Blake).

Sparse Triangular Solver in KokkosKernels (Amesos2 – SuperLU/Tacho)

SuperLU & SpTRSV

- Supernodal LU factorization with partial pivoting
- Triangular solver with **level-set scheduling** (KOKKOSKERNELS); cf. [Yamazaki, Rajamanickam, Ellingwood \(2020\)](#).



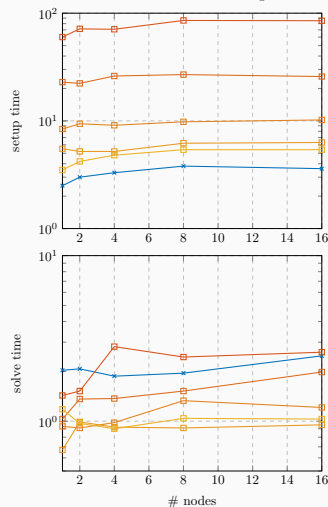
Tacho

- Multifrontal factorization with pivoting inside frontal matrices
- Implementation using KOKKOS using **level-set scheduling**

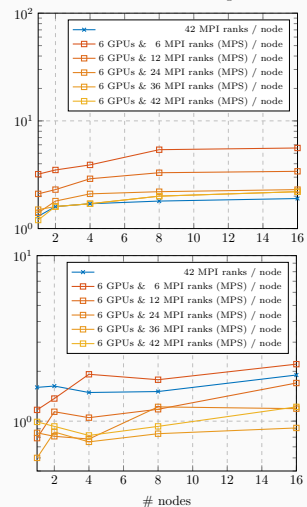
Cf. [Kim, Edwards, Rajamanickam \(2018\)](#).

Three-Dimensional Linear Elasticity – Weak Scalability of FROSch

SUPERLU – weak scaling

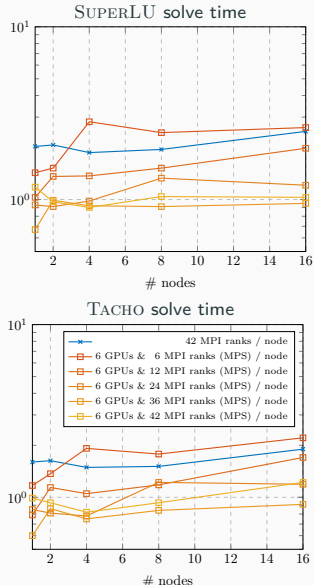


TACHO – weak scaling



Computations on Summit (OLCF): 42 IBM Power9 CPU cores and 6 NVIDIA V100 GPUs per node.
[Yamazaki, Heinlein, Rajamanickam \(2023\)](#)

Three-Dimensional Linear Elasticity – Weak Scalability



Computations on Summit (OLCF): 42 IBM Power9 CPU cores and 6 NVIDIA V100 GPUs per node.

# nodes	1	2	4	8	16
# dofs	375 K	750 K	1.5 M	3 M	6 M
SUPERLU solve					
CPUs	2.03 (75)	2.07 (69)	1.87 (61)	1.95 (58)	2.48 (69)
$n_p/\text{GPU} = 1$	1.43 (47)	1.52 (53)	2.82 (77)	2.44 (68)	2.61 (75)
2	1.03 (46)	1.36 (65)	1.37 (60)	1.52 (65)	1.98 (86)
4	0.93 (59)	0.91 (53)	0.98 (59)	1.33 (77)	1.21 (66)
6	0.67 (46)	0.99 (65)	0.92 (57)	0.91 (57)	0.95 (57)
7	1.03 (75)	1.04 (69)	0.90 (61)	0.97 (58)	1.18 (69)
speedup	2.0×	2.0×	2.1×	2.0×	2.1×
TACHO solve					
CPUs	1.60 (75)	1.63 (69)	1.49 (61)	1.51 (58)	1.90 (69)
$n_p/\text{GPU} = 1$	1.17 (47)	1.37 (53)	1.92 (77)	1.78 (68)	2.21 (75)
2	0.79 (46)	1.14 (65)	1.05 (60)	1.18 (65)	1.70 (86)
4	0.85 (59)	0.81 (53)	0.78 (59)	1.22 (77)	1.19 (66)
6	0.60 (46)	0.86 (65)	0.75 (57)	0.84 (57)	0.91 (57)
7	0.99 (75)	0.93 (69)	0.82 (61)	0.93 (58)	1.22 (69)
speedup	1.6×	1.8×	1.8×	1.6×	1.6×

Yamazaki, Heinlein, Rajamanickam (2023)

Three-Dimensional Linear Elasticity – ILU Subdomain Solver

ILU level		0	1	2	3
setup					
CPU	No	1.5	1.9	3.0	4.8
	ND	1.6	2.6	4.4	7.4
GPU	KK(No)	1.4	1.5	1.8	2.4
	KK(ND)	1.7	2.0	2.9	5.2
	Fast(No)	1.5	1.6	2.1	3.2
	Fast(ND)	1.5	1.7	2.5	4.5
speedup		1.0×	1.2×	1.4×	1.5×
solve					
CPU	No	2.55 (158)	3.60 (112)	5.28 (99)	6.85 (88)
	ND	4.17 (227)	5.36 (134)	6.61 (105)	7.68 (88)
GPU	KK(No)	3.81 (158)	4.12 (112)	4.77 (99)	5.65 (88)
	KK(ND)	2.89 (227)	4.27 (134)	5.57 (105)	6.36 (88)
	Fast(No)	1.14 (173)	1.11 (141)	1.26 (134)	1.43 (126)
	Fast(ND)	1.49 (227)	1.15 (137)	1.10 (109)	1.22 (100)
speedup		2.2×	3.2×	4.3×	4.8×

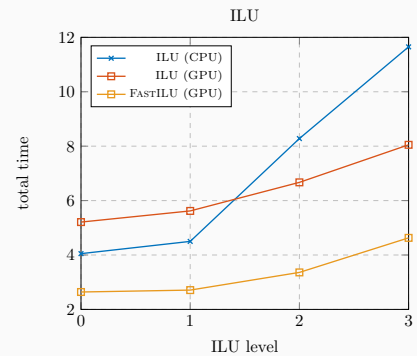
Computations on Summit (OLCF):
42 IBM Power9 CPU cores and 6 NVIDIA
V100 GPUs per node.

Yamazaki, Heinlein,
Rajamanickam (2023)

ILU variants

- KOKKOSKERNELS ILU (KK)
- Iterative FASTILU (Fast); cf. [Chow, Patel \(2015\)](#) and [Boman, Patel, Chow, Rajamanickam \(2016\)](#)

No reordering (**No**) and nested dissection (**ND**)



Three-Dimensional Linear Elasticity – Weak Scalability Using ILU(1)

# nodes	1	2	4	8	16
# dofs	648 K	1.2 M	2.6 M	5.2 M	10.3 M
setup					
CPU		1.9	2.2	2.4	2.4
GPU	KK	1.4	2.0	2.2	2.4
	Fast	1.5	2.2	2.3	2.5
speedup		1.3×	1.0×	1.0×	0.9×
solve					
CPU		3.60 (112)	7.26 (84)	6.93 (78)	6.41 (75)
GPU	KK	4.3 (119)	3.9 (110)	4.8 (105)	4.3 (97)
	Fast	1.2 (154)	1.0 (133)	1.1 (130)	1.3 (117)
speedup		3.3×	3.8×	3.4×	2.5×
speedup			2.6×		

Computations on Summit (OLCF): 42 IBM Power9 CPU cores and 6 NVIDIA V100 GPUs per node.

Yamazaki, Heinlein, Rajamanickam (2023)

Related works

- One-level Schwarz with local solves on GPUs: [Luo, Yang, Zhao, Cai \(2011\)](#)
- Solves of dense local Schur complement matrices in the balancing domain decomposition by constraints (BDDC) method on GPUs: [Šístek & Oberhuber \(2022\)](#)

Learning Extension Operators Using Graph Neural Networks

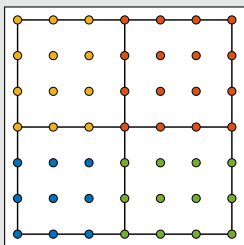
Why Learning Extension Operators

Most coarse spaces for Schwarz preconditioners are constructed based on a **characteristic functions**

$$\varphi_i(\omega_j) = \delta_{ij},$$

on specifically chosen sets of nodes $\{\omega_j\}_j$. The **values in the remaining nodes** are then obtained by **extending the values into the adjacent subdomains**. Examples:

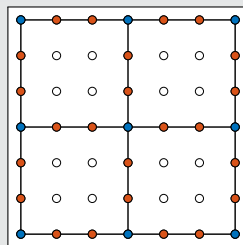
Subdomain-based



- The ω_j are based on nonoverl. subdomains Ω_j
- No extensions needed

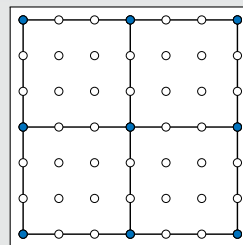
Cf. **Nicolaides (1987)**.

GDSW



- The ω_j are based on partition of the interface
- Energy-minimizing exts.

Vertex-based



- **Lagrangian**: geometric ext.
- **MsFEM**: geometric and energy-minimizing exts.
- **RGDSW**: algebraic and energy-minimizing exts.

Why Learning Extension Operators

Most coarse spaces for Schwarz preconditioners are constructed based on a **characteristic functions**

$$\varphi_i(\omega_j) = \delta_{ij},$$

on specifically chosen sets of nodes $\{\omega_j\}_j$. The **values in the remaining nodes** are then obtained by **extending the values into the adjacent subdomains**. Examples:

Observation 1

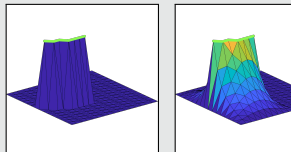
Energy-minimizing extensions

- are **algebraic**:

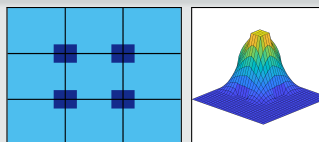
$$v_I = -K_{II}^{-1} K_{I\Gamma} v_\Gamma$$

(with Dirichlet b. c.)

- can be **costly**: solving a problem in the interior



Observation 2

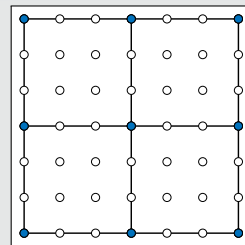


Heterogeneous: $\alpha_{\text{light}} = 1$; $\alpha_{\text{dark}} = 10^8$

The performance may **strongly** depend on extension operator:

coarse space	its.	κ
—	163	$4.06 \cdot 10^7$
Q1	138	$1.07 \cdot 10^6$
MsFEM	24	8.05

Vertex-based



- Lagrangian**: geometric ext.
- MsFEM**: geometric and energy-minimizing exts.
- RGDSW**: algebraic and energy-minimizing exts.

→ Improving efficiency & robustness via machine learning.

Related Works

This overview is **not** exhaustive:

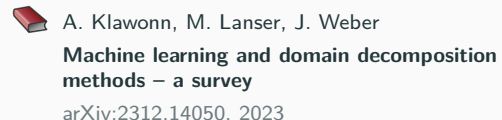
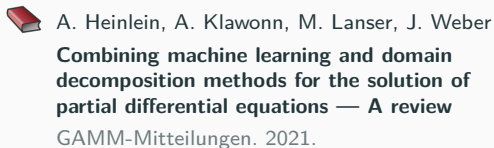
Coarse spaces for domain decomposition methods

- Prediction of the geometric location of adaptive constraints (adaptive BDDC & FETI-DP as well as AGDSW): Heinlein, Klawonn, Langer, Weber (2019, 2020, 2021, 2021, 2021, 2022)
- Prediction of the adaptive constraints: Klawonn, Langer, Weber (preprint 2023, 2024)
- Prediction of spectral coarse spaces for BDDC for stochastic heterogeneities: Chung, Kim, Lam, Zhao (2021)
- Learning interface conditions and coarse interpolation operators: Taghibakhshi et al. (2022, 2023)

Algebraic multigrid (AMG)

- Prediction of coarse grid operators: Luz et al. (2020), Tomasi, Krause (2023)
- Coarsening: Taghibakhshi, MacLachlan, Olson, West (2021); Antonietti, Caldana, Dede (2023)

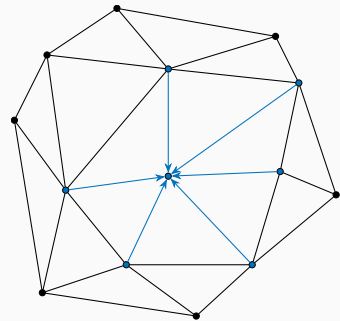
An overviews of the **state-of-the-art** on domain decomposition and machine learning in early 2021 and 2023:



Prediction via Graph Convolutional Networks

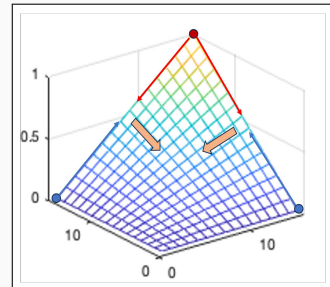
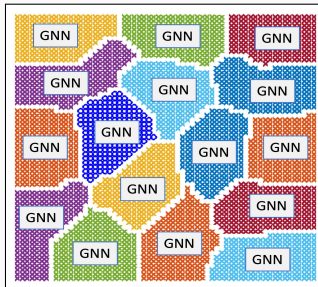
Graph neural networks (GNNs) introduced in **Gori, Monfardini, and Scarselli (2005)** are well-suited for learning on data based on simulation meshes:

- Generalization of classical convolutional neural networks (CNNs) **LeCun (1998)** to graph-based data sets.
- Aggregation and transmission of features of neighboring nodes in the graph via message passing layers.
- Invariance and equivariance with respect to position and permutation of the nodes of the graph.



Local approach

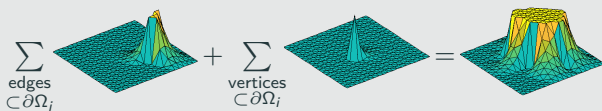
- Input: subdomain matrix K_i
- Output: basis functions $\{\varphi_j^{\Omega_i}\}_j$ on the same subdomain
- Training on subdomains with varying geometry
- Inference on unseen subdomains



Theory-Inspired Design of the GNN-Based Coarse Space

Null space property

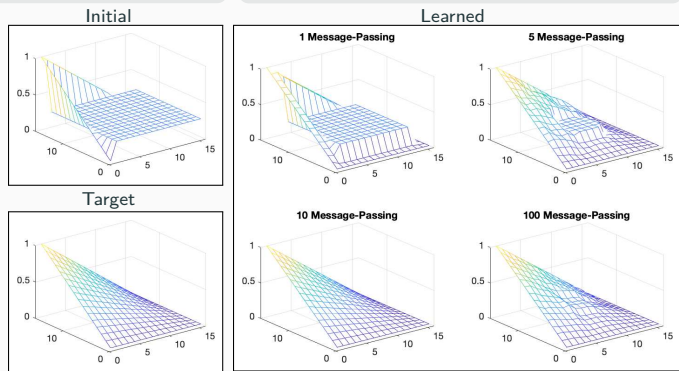
Any extension-based coarse space built from a partition of unity on the domain decomposition interface satisfies the **null space property necessary for numerical scalability**:



Initial and target

- **Initial function:** partition of unity that is constant in the interior
- **Target function:**
 - linear on the edges
 - energy-minimizing in the interior

→ **Information transport via message passing**



Explicit partition of unity

To explicitly enforce that the basis functions $(\varphi_j)_j$ form a **partition of unity**

$$\varphi_j = \frac{\hat{\varphi}_j}{\sum_k \hat{\varphi}_k},$$

where the $\hat{\varphi}_k$ are the outputs of the GNN.

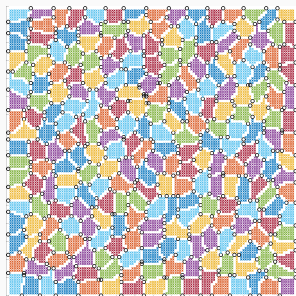
Numerical Results for Homogeneous Laplacian – Weak Scaling Study

Model problem: 2D Laplacian model problem discretized using finite differences on a structured grid

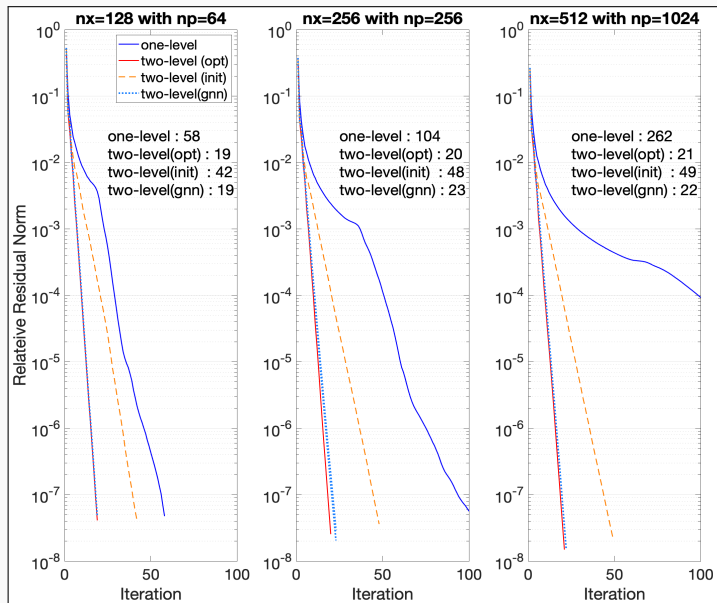
$$-\Delta u = 1 \quad \text{in } \Omega,$$

$$u = 0 \quad \text{on } \partial\Omega,$$

decomposed using METIS:



- The GNN has been trained on 64 subdomains.

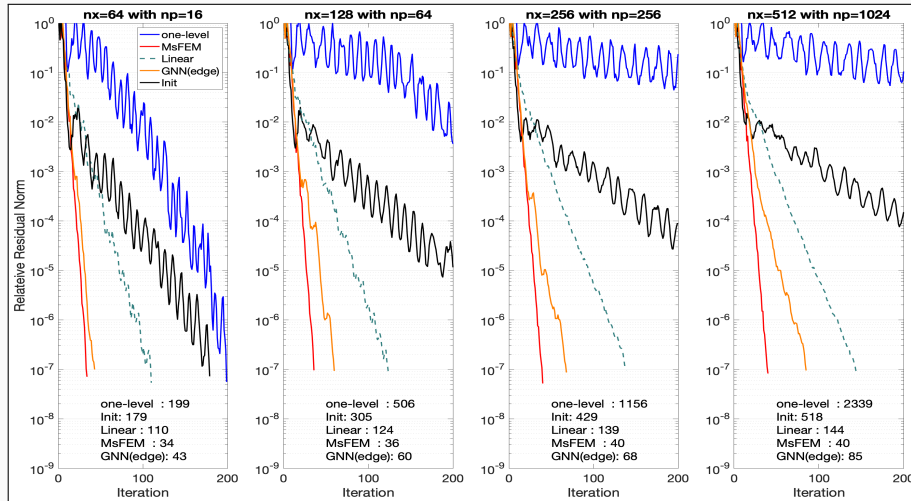


Yamazaki, Heinlein, Rajamanickam (in prep.)

Numerical Results for Heterogeneous Laplacian – Weak Scaling Study

Heterogeneous Laplacian with $\alpha_{\max}/\alpha_{\min} = 10^3$:

$$-\nabla \cdot (\alpha(x) \nabla u(x)) = f \text{ in } \Omega = [0, 1]^2, \quad u = 0 \text{ on } \partial\Omega.$$



Yamazaki, Heinlein, Rajamanickam (in prep.)

FROSCh

- FROSCH is based on the **Schwarz framework** and **energy-minimizing coarse spaces**, which provide **numerical scalability** using **only algebraic information** for a variety of **applications**

Subdomain solves on GPUs

- Subdomain solves make up a **major part of the total solver time**.
- Using the **GPU triangular solve** from KOKKOSKERNELS, we can **speed up** the **solve phase** of FROSCH. It can be **further improved** using **ILU**.

Learning extension operators

- **Extensions** are a major component in the **construction of coarse spaces** for domain decomposition methods.
- Using **GNNs** and **known properties from the theory**, we can **learn extension operators** that lead to a **scalable coarse spaces**.

Thank you for your attention!